

THERMAL EFFECTS OF PHYSICAL HETEROGENEITY IN OLYMPIA UNDAE. N. E. Putzig^{1,†}, L. M. Bowers², M. T. Mellon¹, K. E. Herkenhoff³, and R. J. Phillips¹. ¹Southwest Research Institute, Boulder, CO; ²University of Colorado, Boulder, CO; ³United States Geological Survey, Flagstaff, AZ. † Contact: nathaniel@putzig.com.

Synopsis: The vast dune fields of Olympia Undae exhibit anomalous thermal properties, which led earlier workers to suggest that the dunes are composed of sand-sized agglomerations of dust. More recently, it has been shown that the thermal discrepancy is consistent with ~20 cm of normal basaltic sand overlying shallow ground ice [1,2]. Here, we show that the horizontal mixtures of materials observed in the erg and the slopes of the dune facets are not significant contributors to the thermal behavior. We also find that thermal inertia derived from morning THEMIS images is consistent with that derived from MGS-TES observations and provides a substantial improvement in lateral resolution. Unfortunately, afternoon THEMIS imaging occurs at times of day that precludes deriving unique values of thermal inertia.

Background: Dark dune fields collectively known as the circum-polar erg surround the north polar layered deposits, features which have been linked to climate variations [3,4]. Neutron data suggest that water ice is present within a meter of the erg's surface [5], providing an additional constraint on climate. In Olympia Undae, low values of thermal inertia (~75 tiu, where $\text{tiu} \equiv \text{J m}^{-2} \text{K}^{-1} \text{s}^{-1/2}$) suggestive of dust-sized rather than sand-sized grains are reported from both Viking [6,7] and TES [1]. Dunes of similar morphology, color, and albedo at lower latitudes [8] have thermal inertia (~250 tiu) consistent with sand-sized basaltic grains [9,10,11]. An earlier solution to this discrepancy involving the bonding of fines into larger, low-density aggregate particles capable of forming dunes [12,13] has been obviated by the revelation from thermal models [14,15] that heterogeneous surfaces may produce anomalous thermal behavior, including apparent thermal inertia values lower than the intrinsic thermal inertia of model components. Thus, the current explanation for the thermal properties of the erg allows that they are in fact formed of ordinary basaltic sand (perhaps with a varying admixture of gypsum [16]) that is ice-cemented at depth with an ice-free surface layer. This geometry is capable of producing very low values of apparent thermal inertia [17,1].

Horizontal heterogeneity in Olympia Undae:

While the earlier modeling work [1] included a qualitative assessment of the thermal effects of horizontal mixtures of materials, a more quantitative analysis and the inclusion of the effects of slope was needed to evaluate the thermal effects of these features.

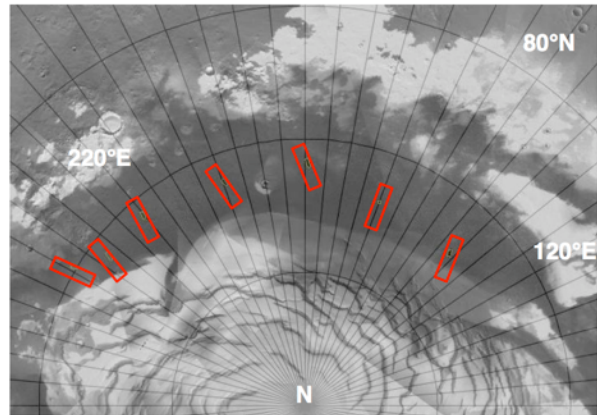


Figure 1. Location map of HiRISE images within Olympia Undae. Background is MOC wide-angle mosaic overlain on MOLA shaded relief. From [18].

Using a representative set of HiRISE images of the erg (e.g., Fig. 1), we measured the relative area of light-toned inter-dune deposits and the orientation of crest lines (Fig. 2). MOLA data and terrestrial observations were used to constrain the dune-face slope angles (a HiRISE DEM for the dunes should be available soon). Interdune deposits cover ~2–8% of the surface area and crest lines are consistently oriented across Olympia Undae at an azimuth of $350^\circ \pm 20^\circ$. MOLA provides a lower bound on slope angle of 2° – 3° and terrestrial studies show angles of repose anywhere from 15° to 45° , depending on the dune materials.

The small area of interdune deposits will have a minimal effect on apparent thermal inertia [14]. Depending on the slope angle, the geometry of the dunes will have a more substantial effect. However, we

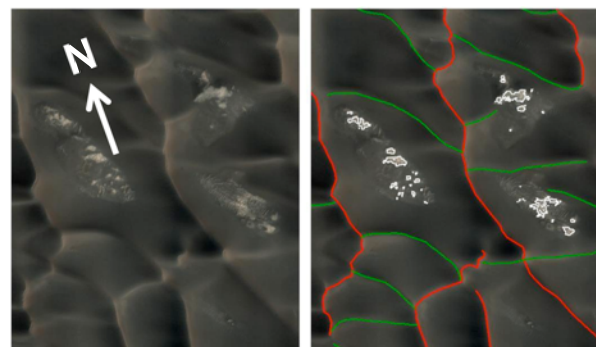


Figure 2. Section of HiRISE image PSP_001432_2610 showing dune crests and inter-dune deposits within Olympia Undae. From [18].

find that potential deviations in apparent thermal inertia induced by slopes oriented as those in the erg have the opposite sense to the observed values (Fig. 3). Thus, these other forms of heterogeneity are not major factors, and the layering of dry sand over an ice-cemented substrate remains the most viable explanation of the observed thermal behavior.

THEMIS thermal inertia: At 100 m/pixel, THEMIS images provide higher spatial resolution than TES (~3 km/pixel), and may enable better discrimination between heterogeneity models. To that end, we derived thermal inertia from THEMIS Band 9 images of Olympia Undae. In earlier work, we had found that such THEMIS results were equivocal [1], with morning observations showing only a rough correlation to TES results and afternoon observations producing extremely high values of doubtful accuracy. In 2009, the Mars Odyssey orbit was moved to an earlier local time, with equator crossings now at about 3:30AM and 3:30PM. During Mars Year 30, the first after the orbit change, afternoon images were acquired over a broad range of seasons, but morning imaging was restricted to late summer (L_s 171–182). Upon deriving thermal inertia for the new images, we find that the afternoon results remain of little use. The erg’s high latitude and the spacecraft’s inclination combine to place local times near 5:15PM, still a poor time of day for thermal inertia derivation (Fig. 4). Despite the restricted season of the morning images, we find a good correspondence between their results and those of TES at the same season (Fig. 5). Thermal modeling suggests that CO₂ may be freezing diurnally at these seasons (Fig. 4). We have requested acquisition of morning THEMIS images in MY31 during L_s 140–160, hoping to obtain more optimal seasonal coverage.

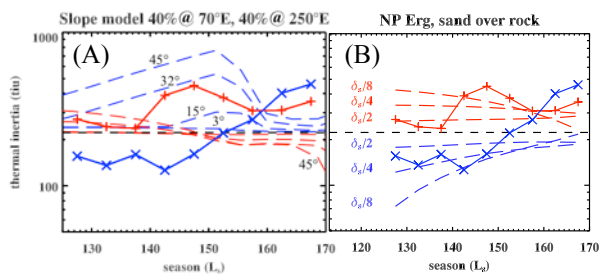


Figure 3. Seasonal apparent thermal inertia as derived from TES data (solid lines and symbols) and as derived from model dune surfaces for the site shown in Fig. 2. (A). Models with various slope angles. Deviations from the model sand value (225 tiu) are progressively larger for greater slope angles, and the sense of deviation for nightside (blue) and dayside (red) differs strongly from the TES-observed behavior, indicating that the dune slopes are not responsible for the thermal anomaly. (B). Models with various thicknesses of dry sand over “rock” (i.e., ice-cemented sand). Best fit to TES data is a dry layer of $\sim \delta_s/4$ (18 cm).

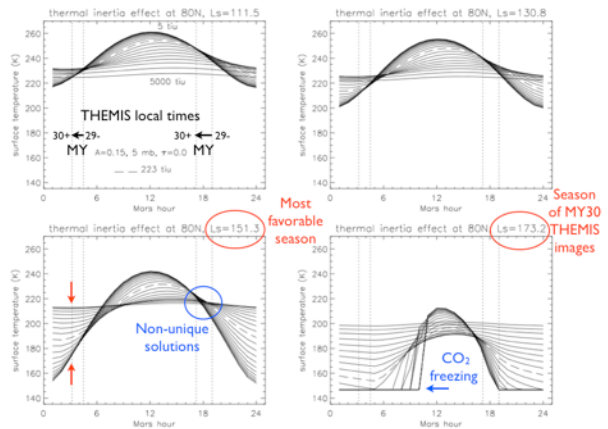


Figure 4. Model temperature at 80°N for a range of thermal inertia at 4 seasons. THEMIS PM image times yield non-unique solutions before and after the Odyssey orbit change. The optimal season for morning images is near L_s 150 when curve separations are greatest (red arrows). AM imaging in MY30 may include frost cover for surfaces of low thermal inertia (blue arrow).

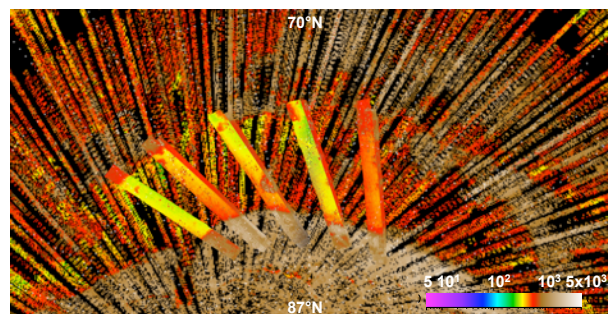


Figure 5. Map of apparent thermal inertia as derived from TES data (background) for L_s 170–180, overlain with images of thermal inertia derived from morning (~3:15AM) THEMIS images acquired in Mars Year 30.

References: [1] Putzig N.E. et al. (2010) *Second Dunes Workshop*, LPI Cont. No 2037. [2] Titus T.N. et al. (2011) *Fifth Mars Polar Sci. Conf.*, LPI Cont. No. 1323.[3] Thomas P. et al. (1992) in: *Mars*, Kieffer H.H. et al. (1992) U. AZ Press. [4] Clifford S.M. et al. (2000) *Icarus 144*, 210–242. [5] Feldman W.C. et al. (2008) *Icarus 196*, 422-432. [6] Paige D.A. et al. (1994) *JGR 99*, 25,959–25,991. [7] Vasavada A.R. et al. (2000) *JGR 105*, 6961–6969.[8] Thomas P. & Weitz C. (1989) *Icarus 81*, 185-215. [9] Sagan C. & Bagnold R.A. (1975) *Icarus 26*, 209-218. [10] El-Baz F. et al. (1979) *JGR 84*, 8205-8221. [11] Breed C.S. et al. (1979) *JGR 84*, 8183-8204. [12] Herkenhoff K.E. & Vasavada A.R. (1999) *JGR 104*, 16,487–16,500. [13] Cutts J.A. et al. (1976) *Science 194*, 1329-1337. [14] Putzig N.E. & Mellon M.T. (2007) *Icarus 191*, 52-67. [15] Mellon M.T. & Putzig N.E. (2007) *LPS XXXVIII*, Abstract #2184. [16] Horgan et al. (2009) *JGR 114*, E01005. [17] Putzig N.E. & Mellon M.T. (2007) *Icarus 191*, 68-94. [18] Bowers L.M. and Putzig N.E (2011) *LPS LXII*, Abstract 2819.